

Fast Methods for Approximation of Resolution and Covariance for SPECT

J. Webster Stayman, *Student Member, IEEE*, and Jeffrey A. Fessler, *Member, IEEE*

Abstract—Resolution and covariance predictors have been derived previously for penalized-likelihood estimators. These predictors can provide accurate approximations to the local resolution properties and covariance functions for tomographic systems given a good estimate of the mean measurements. However, when numerous evaluations are made repeatedly (as in penalty design or calculation of variance images), these predictors still require large amounts of computing time. In [1], we discussed methods for precomputing a large portion of the predictor for shift-invariant system geometries. In this paper, we generalize the efficient procedure discussed in [1] to shift-variant single photon emission computed tomography (SPECT) systems. This generalization relies on a new attenuation approximation and several observations on the symmetries in SPECT systems. These new general procedures apply to both 2D and fully-3D SPECT models, that may be either precomputed and stored, or written in procedural form.

Index Terms—Tomography, local impulse response, noise, variance, image quality.

I. INTRODUCTION

EQUATIONS for predicting the mean and variance have been derived in [2] and for predicting resolution properties in [3]. These predictions have been applied to several applications including penalty design for uniform resolution [1], [4], and contrast optimization [5], and with computer observer models [6]. While resolution and noise prediction has potential uses across a range of applications, the evaluation of these predictions is computationally expensive. This paper investigates a number of approximations that make these evaluations more practical.

Approximations for noise and resolution prediction have been used in [7] that yield practical computation times. However, when very many evaluations are required (*e.g.*: when resolution predictions are made for every pixel position, or noise predictions are made repeatedly for different reconstruction parameters or objects), the computational burden is still high. Generally, the dominant computation is the calculation of repeated weighted backprojections of projection data. In some cases, as in an idealized PET system where the system response is space-invariant, computation time can be reduced through an appropriate factorization and precomputation (see [1]). However such methods are inapplicable to space-variant systems, such as for SPECT with a depth-dependent detector response. We have previously investigated fast methods for cases where the space-variant system may be modeled with

a precomputed system matrix [4]. Such methods are generally impractical for 3D systems, where the system model is too large to be precomputed and stored. Other attempts at reducing calculation time have been made using approximations based on approximating the SPECT model using a space-invariant model [8].

In this paper, we discuss a technique for making noise and resolution predictions that are appropriate for both 2D and fully 3D SPECT systems. These methods are appropriate for systems where projections and backprojections are done “on-the-fly”, and apply generally to noncircular orbits and nonuniform attenuation. The approach discussed here is an extension of the linear operator approach discussed in [1] for PET systems. We apply approximations that reduce storage and computation, yet retain prediction accuracy.

II. BACKGROUND

Consider the following SPECT model, where the measurement vector, $\underline{Y} = [Y_1, \dots, Y_N]$, is related to the emission image, $\underline{\lambda} = [\lambda_1, \dots, \lambda_P]$, through their means as follows

$$\bar{\underline{Y}}(\underline{\lambda}) = \mathbf{H}\underline{\lambda} + \underline{r}, \quad (1)$$

where $\mathbf{H} \in \mathbb{R}^{N \times P}$ is the system matrix, and $\underline{r} = [r_1, \dots, r_N]$ represents the mean contribution from scatter and background events. In SPECT, usually one can factor elements of \mathbf{H} , as $h_{ij} = b_i g_{ij} a_{ij}$, where b_i denotes ray-dependent factors that incorporate nonuniformities across the face of the detector, $\mathbf{G} = \{g_{ij}\}$ represents an object-independent geometric system model, and $\mathbf{A} = \{a_{ij}\}$ describes the object-dependent attenuation effects into the model. Using matrices, we write $\mathbf{H} = \mathbf{D}_B(\mathbf{A} \odot \mathbf{G})$, where \mathbf{D}_B is a diagonal matrix with elements b_i .

We reconstruct the emission image from the measurements using a penalized-likelihood estimator defined as the implicit maximizer of an objective function,

$$\hat{\underline{\lambda}} = \arg \max L(\underline{\lambda}, \underline{Y}) - R(\underline{\lambda}), \quad (2)$$

where the objective function is written as the difference of a log-likelihood term, $L(\underline{\lambda}, \underline{Y})$, and a penalty term, $R(\underline{\lambda})$.

Using the formulations in [2] and [3], and the circulant approximations in [7], one may quantify the resolution properties of $\hat{\underline{\lambda}}$ using an approximation for the local impulse response,

$$\underline{l}^j = \mathcal{F} \left\{ \frac{\mathcal{F} \{ \mathbf{H}' \mathbf{D} \mathbf{H} \underline{e}^j \}}{\mathcal{F} \{ \mathbf{H}' \mathbf{D} \mathbf{H} \underline{e}^j + \mathbf{R}(\underline{\lambda}) \underline{e}^j \}} \right\}, \quad (3)$$

This work was supported in part by NSF grant BES-9982349 and by NIH grant CA-60711.

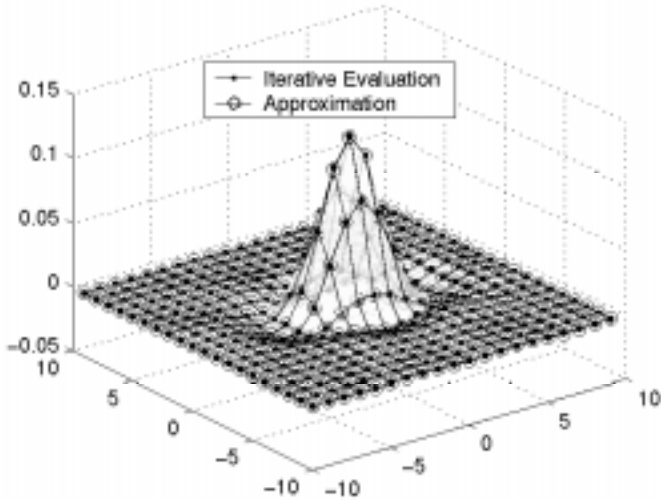


Fig. 1. Our local impulse response approximation versus a response calculated using the iterative methods described in [3].

and the covariance approximation,

$$\text{Cov}^j\{\hat{\lambda}\} = \mathcal{F} \left\{ \frac{\mathcal{F}\{H'DH\underline{e}^j\}}{[\mathcal{F}\{H'DH\underline{e}^j + \mathbf{R}(\lambda)\underline{e}^j\}]^2} \right\}. \quad (4)$$

In these two equations, $\mathcal{F}\{\cdot\}$ represents the Fourier transform of its vector argument, $\mathbf{R}(\lambda)$ is the Hessian of the penalty function, and \underline{e}^j is the j th unit vector that indicates the position of the local response or covariance function. Under a Poisson model for the measurements, we use a diagonal weighting matrix [3], $\mathbf{D} = \text{diag}\{1/Y_i\}$.

Because the Fourier transforms can be calculated quickly using fast Fourier transforms, the computations are dominated by calculating the weighted projection-backprojection, $H'DH\underline{e}^j$. Fast calculation of this term is the key to efficient evaluation of the noise and resolution predictions.

III. EFFICIENT CALCULATION OF $H'DH\underline{e}^j$

We have previously investigated a technique for efficient calculation of $H'DH\underline{e}^j$ when H models a shift-invariant PET system [1]. This technique was based on replacing $H'DH\underline{e}^j$ with an object-independent matrix that operates on the diagonal elements of \mathbf{D} . Specifically, since $H'DH\underline{e}^j$ is linear in the elements of \mathbf{D} , one may find a set of linear operators, \mathbf{M}^j , such that,

$$H'DH\underline{e}^j = \sum_{i=1}^N m_i^j [D]_{ii} = \mathbf{M}^j \underline{d}, \quad (5)$$

where $\underline{d} \in \mathbb{R}^N$ is a vector of the diagonal elements of \mathbf{D} . We construct columns of \mathbf{M}^j , using superposition with $\underline{m}_i^j = H' \text{diag}\{\underline{e}^i\} H \underline{e}^j$. Unfortunately, for SPECT these operators are *object-dependent* because of attenuation. Thus precomputation of these operators generally does not provide a useful speed-up for SPECT.

To find a suitable approach for SPECT, consider the following observations. Letting $\mathbf{F} = H'DH$, we write the (k, j) th element of \mathbf{F} as

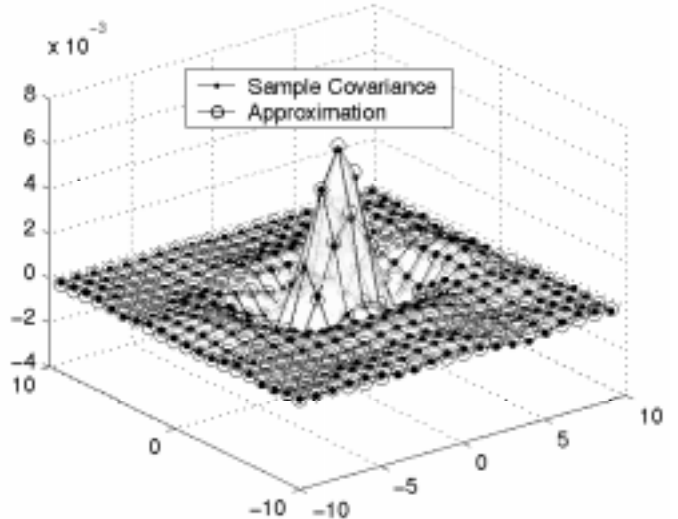


Fig. 2. Comparison of covariance approximation versus an estimate formed by calculating the sample covariance over 1000 reconstructions.

$$\begin{aligned} [\mathbf{F}]_{kj} &= (\underline{e}^k)' \mathbf{F} \underline{e}^j = (\underline{e}^k)' H' D H \underline{e}^j \\ &= (\underline{e}^k)' [D_B (\mathbf{A} \odot \mathbf{G})]' \mathbf{D} [D_B (\mathbf{A} \odot \mathbf{G})] \underline{e}^j \\ &= [(\mathbf{A} \underline{e}^k)' \odot (\mathbf{G} \underline{e}^k)]' \mathbf{D}_B \mathbf{D} \mathbf{D}_B [(\mathbf{A} \underline{e}^j) \odot (\mathbf{G} \underline{e}^j)] \\ &= (\mathbf{G} \underline{e}^k)' \text{diag}\{\mathbf{A} \underline{e}^k\} \mathbf{D}_B \mathbf{D} \mathbf{D}_B \text{diag}\{\mathbf{A} \underline{e}^j\} \mathbf{G} \underline{e}^j \\ &= (\underline{e}^k)' \mathbf{G}' \mathbf{D}^{jk} \mathbf{G} \underline{e}^j, \end{aligned} \quad (6)$$

where the diagonal matrix, \mathbf{D}^{jk} , has the following elements

$$[\mathbf{D}^{jk}]_{ii} = [\mathbf{A} \underline{e}^k]_i [\mathbf{D}]_{ii} [D_B]_{ii}^2 [\mathbf{A} \underline{e}^j]_i = b_i^2 a_{ij} a_{ik} [\mathbf{D}]_{ii}. \quad (7)$$

Because $\mathbf{A} \underline{e}^k$ generally varies relatively smoothly with changing k and $H'DH\underline{e}^j$ is fairly concentrated about the pixel position j , we make the following approximation,

$$\mathbf{F} \underline{e}^j = H'DH\underline{e}^j \approx \mathbf{G}' \mathbf{D}^{jj} \mathbf{G} \underline{e}^j. \quad (8)$$

Thus, we have an approximation where the object-dependence enters only through the diagonal weighting (as in the PET case discussed in [1]). The approximation (8) is *exact* at position j and yields good predictions for a neighborhood around j . Because of the object-independence of \mathbf{G} , we precompute the following object-independent linear operators

$$\hat{\mathbf{m}}_i^j = \mathbf{G}' \text{diag}\{\underline{e}^i\} \mathbf{G} \underline{e}^j. \quad (9)$$

With these precalculated, we form predictions using

$$H'DH\underline{e}^j \approx \hat{\mathbf{M}}^j \hat{\underline{d}}^j, \quad (10)$$

where elements of $[\hat{\underline{d}}^j]_i = b_i^2 a_{ij}^2 [\mathbf{D}]_{ii}$.

While (10) represents the key approximation that we use in approximating $H'DH\underline{e}^j$, we have developed additional simplifications that reduce storage and computation making the evaluation of $H'DH\underline{e}^j$ via (10) practical. These additional simplifications are discussed in greater detail in [9].

IV. RESULTS

Because the precalculation of (9) involves significant computation time, the main advantage of our methods over other

techniques arises when one wants to repeatedly calculate the weighted projection-backprojection for different diagonal weightings. Therefore, if one wants to investigate covariance functions for many different images, or one wants to be able to design a object-dependent shift-variant penalty as in [1] or [5], our approximation will greatly reduce computation time. While this is the main advantage, when one uses the additional approximations we have derived (but not discussed in this short summary), it is possible to reduce computation time versus traditional predictors even when one includes precomputation times in the comparison.

To illustrate the potential utility and accuracy of our approximation, we have compared sample local impulse responses and covariance functions using our new approximations and more traditional methods. Figure 1 compares our approximate local impulse response using methods based on (10) and (3), versus the iterative approach described in [3] (using the true \mathbf{H}). These methods yield nearly indistinguishable results although the approximate method takes a very small fraction of the time of the iterative approach. One obtains similar accuracy using the circulant approach in (3). However, compared to our method (when the linear operators have already been precalculated) the computational burden is much greater than our approach.

Figure 2 compares covariance functions with similar conclusions. Our approximation, using (10) and (4), matches very well with an empirically calculated covariance and, for precomputed operators, the computation time is greatly reduced compared to other prediction methods.

REFERENCES

- [1] J. W. Stayman and J. A. Fessler, "Regularization for uniform spatial resolution properties in penalized-likelihood image reconstruction," *IEEE Tr. Med. Im.*, vol. 19, pp. 601–15, June 2000.
- [2] J. A. Fessler, "Mean and variance of implicitly defined biased estimators (such as penalized maximum likelihood): Applications to tomography," *IEEE Tr. Im. Proc.*, vol. 5, pp. 493–506, Mar. 1996.
- [3] J. A. Fessler and W. L. Rogers, "Spatial resolution properties of penalized-likelihood image reconstruction methods: Space-invariant tomographs," *IEEE Tr. Im. Proc.*, vol. 5, pp. 1346–58, Sept. 1996.
- [4] J. W. Stayman and J. A. Fessler, "Compensation for nonuniform resolution using penalized-likelihood reconstruction in space-variant imaging systems," *IEEE Tr. Med. Im.*, 2002. accepted.
- [5] J. Qi and R. M. Leahy, "A theoretical study of the contrast recovery and variance of MAP reconstructions with applications to the selection of smoothing parameters," *IEEE Tr. Med. Im.*, vol. 18, pp. 293–305, Apr. 1999.
- [6] P. Bonetto, J. Qi, and R. M. Leahy, "Covariance approximation for fast and accurate computation of channelized Hotelling observer statistics," *IEEE Tr. Nuc. Sci.*, vol. 47, pp. 1567–72, Aug. 2000.
- [7] J. Qi and R. M. Leahy, "Resolution and noise properties MAP reconstruction for fully 3D PET," *IEEE Tr. Med. Im.*, vol. 19, pp. 493–506, May 2000.
- [8] Y. Xing, I. T. Hsiao, and G. R. Gindi, "Efficient calculation of resolution and variance in 2D circular-orbit SPECT," in *Proc. IEEE Nuc. Sci. Symp. Med. Im. Conf.*, pp. M5B–5, 2001.
- [9] J. W. Stayman and J. A. Fessler, "Efficient calculation of resolution and covariance for fully 3D SPECT," *IEEE Tr. Med. Im.*, 2002. submitted.